

Interference investigations of liquid crystal–polymer composites structure

PETER MAKSYMYAK¹, ANDRIY NEGRYCH^{1*}, LEONID DOLGOV², OLEG YAROSHCHUK²

¹Correlation Optics Dept, Chernivtsi University, 2 Kotsyubinsky Str., Chernivtsi, 58012, Ukraine

²Institute of Physics, NASU, pr. Nauki 46, Kyiv, 03028, Ukraine

*Corresponding author: nehrych@itf.cv.ua

The methods of correlation optics are for the first time applied to study the structure of liquid crystal–polymer (LC–P) composites. Their phase correlation function (PCF) was obtained considering LC–P composite as a random phase screen. The amplitude of PCF contains information about the number of LC domains and structure of LC director inside of them, while a half-width of this function is connected with the size of these domains. In good agreement with previous studies by SEM technique we detected a monotone decrease of LC domains with polymer concentration. When applying the electric field, for the samples with $\varphi_p > 35$ vol.% (PDLC morphology), the amplitude of PCF is monotonic. On the contrary, if $\varphi_p < 35$ vol.% (PNLC morphology) the amplitude of PCF is non-monotonic and, depending on the applied voltage, goes through maximum.

Keywords: liquid crystal, PDLC, light scattering, correlation optics, phase correlation function, morphology.

1. Introduction

Liquid crystal–polymer (LC–P) composite systems are of great practical interest for several reasons. First, polymer network stabilizes desirable LC textures and eliminates parasitic backflow effect in electro-optic LC cells. Second, at high polymer concentration, LC–P composites scatter light intensively. The light scattering amplitude can be effectively controlled by electric field. The structural evolution of LC–P composites with the concentration of polymer phase is an interesting academic question, which might explain concentration behavior of electro-optical, optical and dielectric characteristics. Earlier we studied this problem by optical and scanning electron microscopy (SEM) [1, 2]. In these experiments LC–P samples were kept in alcohol to dissolve LC, then dried and coated by conductive film. In fact, SEM allowed us to study only morphology of polymer phase, which can be substantially deformed in the course of sample preparation for this technique. In view of this, there is a strong need for non-destructive methods for the structural studies of this system. In the present

paper, we show that methods of correlation optics, earlier approved for other objects [3, 4], are rather useful for this purpose. Considering LC–P composite as a random phase screen these methods deal with a phase correlation function (PCF) of this screen. PCF contains information about scatter's shape and size, *i.e.*, about parameters of LC domains in the case of LC–P composites. The data obtained by this technique are supported by results of optical microscopy. Good correlation between the data obtained by these methods and earlier results of SEM studies proves good reliability of the new approach.

2. Experiment

2.1. Fundamentals of the method

The layer of LC–P composite is the phase-inhomogeneous object, in which both liquid crystal and polymer contribute to the resulting phase inhomogeneities. The statistical parameter characterizing phase inhomogeneity of the LC–P as a whole is considered to be the phase variance of its boundary field. Integral fluctuations of the index of refraction may be estimated through determining a correlation function of the LC–P's phase inhomogeneities. We propose to do this by measuring the transverse coherence function of the field passing the cell [4].

The consideration is based on the model of random phase screen (RPS) [5] presuming: *i*) infinite extension of the object, *ii*) smoothness of inhomogeneities, and *iii*) phase variance less than unity $\sigma^2 < 1$. If the phase fluctuations are statistically homogeneous and obey the Gaussian statistics, then there exists the following interrelation between the correlation characteristics of an RPS and the transverse coherence function of the field $\Gamma(\rho)$ [4]:

$$\Gamma(\rho) = \exp\left\{\sigma^2 [K_s(\rho) - 1]\right\} = \exp\left\{-0.5 D_s(\rho)\right\} \quad (1)$$

where $K_s(\rho)$ is the phase correlation coefficient of the screen's boundary field, $\sigma^2 K_s(\rho)$ is the transverse coherence function of the phase $\Psi_s(\rho)$ and $D_s(\rho)$ is the phase structure function.

We performed the measurements using the arrangement shown in Fig. 1. The He-Ne laser beam ($\lambda = 632.8$ nm, $P = 55$ mW) passes through the inverse telescopic system T which forms a plane wave front. Radiation scattered by the object is divided into an amplitude-splitting interferometer in two components of equal amplitudes. Then relative transversal shift of these components and collinear mixing of them at the interferometer output are provided. The objective MO images any cross-section of the scattered field into the field-of-view diaphragm (FD). The registered frequency spectrum is controlled using the aperture diaphragm (AD). Transversal shift ρ of two beam components is controlled by adjusting one of the mirrors. Then the visibility of interference pattern, $V = (I_{\max} - I_{\min})/(I_{\max} + I_{\min})$, is measured. These measurements were performed for the unpowered LC–P samples and for the samples under

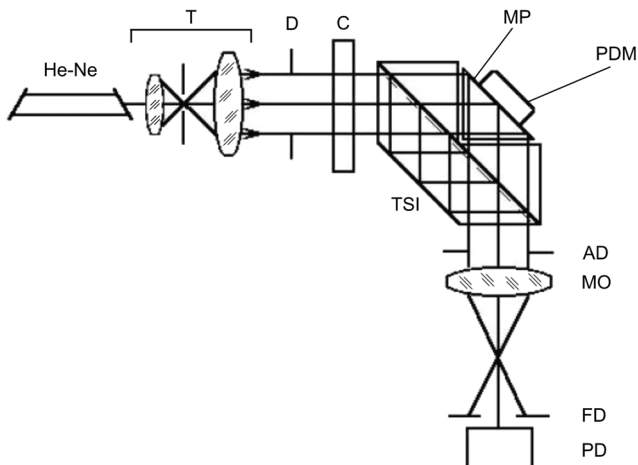


Fig. 1. Experimental arrangement: He-Ne – laser, T – inverse telescopic system, D – diaphragms, C – cell, TSI – transverse-scanning interferometer, MP – movable prism, PDM – prism displacement mechanism, FD – field-of-view diaphragm, MO – microobjective, AD – aperture diaphragm, PD – photodetector.

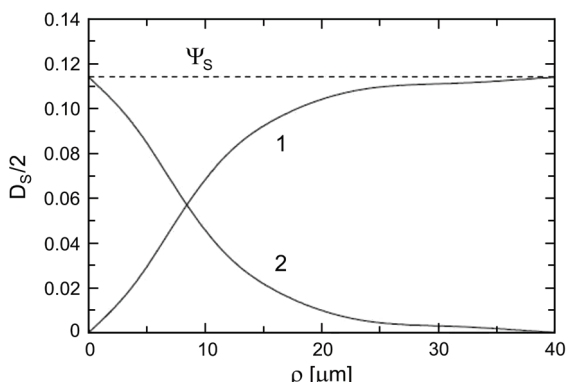


Fig. 2. Typical behavior of the structure function (curve 1) and the phase correlation function (curve 2).

electric field with different polymer concentrations. The electric field was applied to the composite cells using transparent ITO electrodes deposited on the internal surfaces of the glass substrates.

Here, I_{\max} and I_{\min} are intensities of the resulting field for optical path differences of the mixed components $2m\lambda/2$ and $(2m+1)\lambda/2$ (m is integer), respectively. If the interfering beams are of equal intensities, the visibility is equal to the coherence degree of the resulting field. The dependence $\Gamma(\rho)$ obtained in such a manner is used for determining a phase variance σ^2 and the phase correlation coefficient $K_s(\rho)$ shown in Fig. 2 for the typical phase object. Taking the logarithm of the ratio (1), one obtains:

$$\ln[\Gamma(\rho)] = \sigma^2 [K_s(\rho) - 1] = -0.5 D_s(\rho) \quad (2)$$

The region where $D_s(\rho)$ saturates corresponds to $K_s(\rho) = 0$. The ordinate of the saturation region gives the value of phase variance of the object boundary field σ^2 . Using the dependence $0.5D_s(\rho)$ and knowing σ^2 , one can determine the correlation function of phase inhomogeneities $\Psi_s(\rho)$.

2.2. Samples

The LC-P samples were prepared on the base of nematic LC E7 from Merck and photopolymer NOA65 from Norland. These components are proven to form good match for PDLC composites [1, 6, 7]. The polymer concentration was varied from 10 to 35 vol.%. The components were thoroughly mixed. Then a drop of mixture was placed on ITO covered glass slab and pressed with the other ITO coated glass slab. The gap between the slabs, *i.e.*, the thickness of suspension layer, was maintained by 5 μm spacers. The cell was glued by an epoxy glue and then subjected to UV irradiation from high pressure mercury lamp. The light intensity and exposure time were 90 mW/cm² and 20 min, respectively. In electro-optic experiments, samples were powered by sine like alternative voltage ($U < 150 \text{ V}$, $f = 1 \text{ kHz}$).

3. Results and discussion

Figures 3–5 shows phase inhomogeneities correlation functions $\Psi_s(\rho)$ for the composites with 10, 15 and 20 vol.% of polymer. The $\Psi_s(\rho)$ curves are presented for non-powered state and for the states corresponding to different intensities of external electric field.

Taking into consideration the data for samples of all concentrations the following regularities can be observed:

1. The half-width of $\Psi_s(\rho)$, connected with scatters' size, monotonically decreases with polymer concentration. Figure 6 shows the phase correlation coefficient $K_s(\rho)$ for LC-P composite with 10, 15, 20 and 25 vol.% of polymer for voltage on cell which correspond to maximum phase variance.

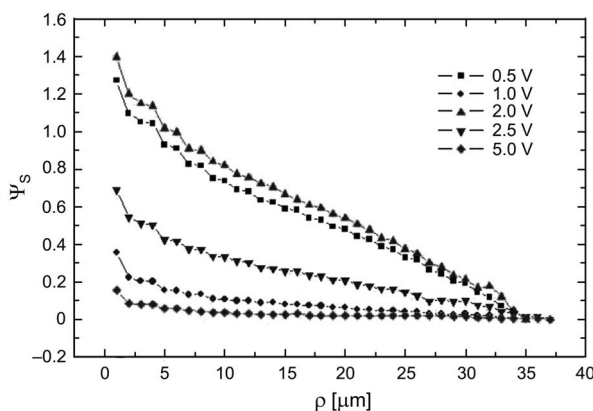


Fig. 3. Correlation functions of phase inhomogeneities for LC-P composite with 10 vol.% of polymer.

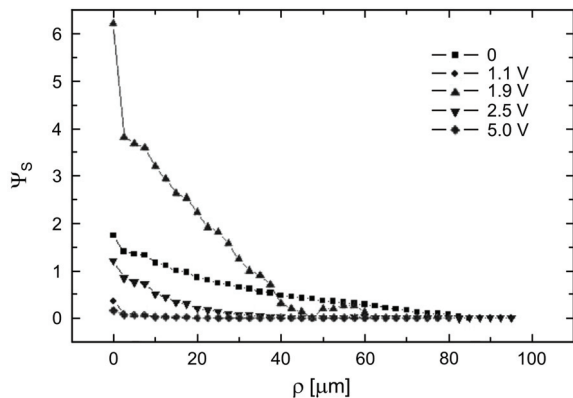


Fig. 4. Correlation functions of phase inhomogeneities for LC-P composite with 15 vol.% of polymer.

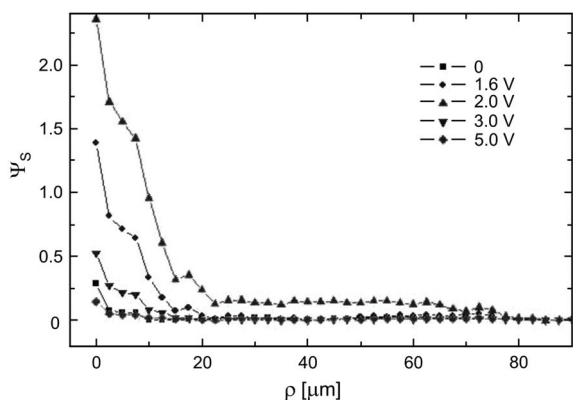


Fig. 5. Correlation functions of phase inhomogeneities for LC-P composite with 20 vol.% of polymer.

For LC-P composite with 10, 15, 20 and 25 vol.% of polymer we obtained the following values of the half-width of phase correlation coefficient: 32, 20, 8 and 3 μm . This is in good agreement with the size of LC domains estimated by scanning electron microscopy [2]. A monotonic decrease of LC domains with concentration of polymer phase is also confirmed by sample observation in polarizing microscope.

Visual estimations were made on the basis of microscopic images. We have chosen on the photos the field of vision which has an area of $300 \times 200 \mu\text{m}^2$. In Figure 7, microphotographs of phase separation for LC-P composite with 10, 15, 20 and 25 vol.% of polymer are shown.

2. Phase coherence function Ψ_s monotonically decreases with applied voltage. This is caused by strong reduction of the amount of scatters with the applied voltage, because of orientation of LC domains along the field. The amplitude of PCF, proportional to the phase variance σ^2 , as discussed above, behaves differently with a change of voltage for the samples with different polymer content. For the samples with $\varphi_P > 30$ vol.% (samples having morphology of polymer dispersed LC), this

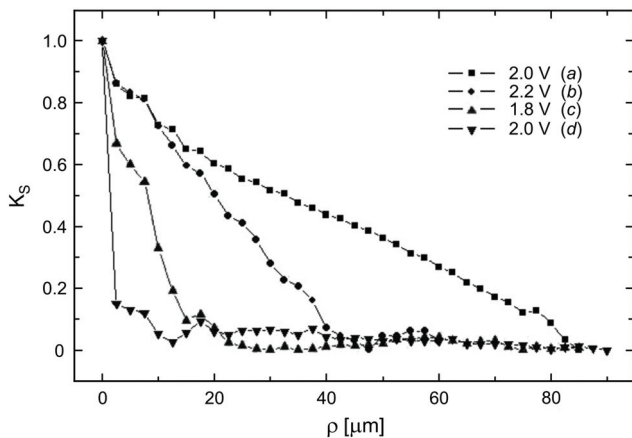


Fig. 6. Phase correlation coefficient for LC–P composite with 10 vol.% (a), 15 vol.% (b), 20 vol.% (c) and 25 vol.% (d) of polymer.

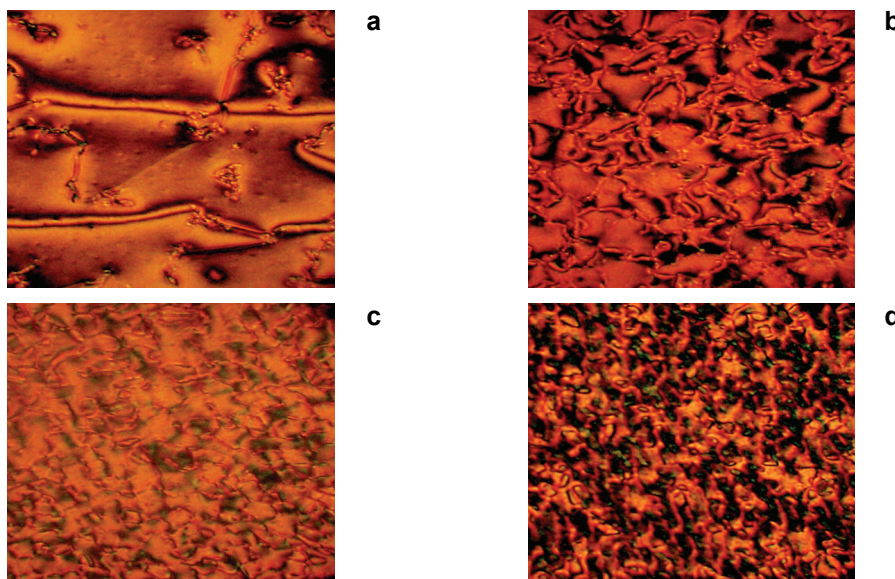


Fig. 7. Microphotographs for LC–P composite with 10 vol.% (a), 15 vol.% (b), 20 vol.% (c) and 25 vol.% (d) of polymer.

dependence is quasi-monotonic (see Fig. 8). In turn, if $\varphi_P < 30$ vol.% (samples with polymer network LC morphology), the amplitude of PCF non-monotonically depends on the applied voltage going through a maximum (see Figs. 9 and 10).

A similar effect earlier observed for samples with PDLC morphology was explained by interference of light passed through the LC droplets and between them [8]. In our case, in contrast to [8], samples have morphology of polymer network

liquid crystal. We think that maximum of phase dispersion σ^2 is caused by a sequence of transformations of orientational defects with the increase of electric fields, which can be easily observed in polarizing microscope. These structural changes can be

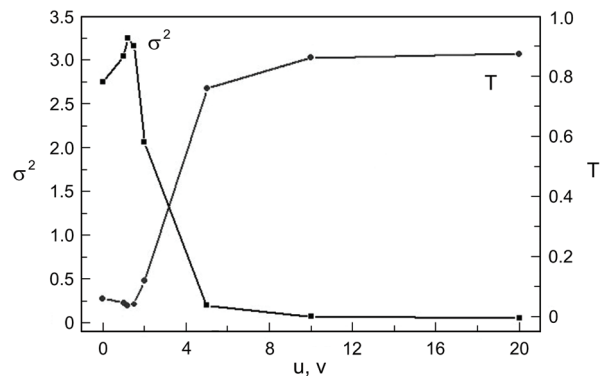


Fig. 8. Phase dispersion σ^2 and transmittance T for LC-P composite with 35 vol.% of polymer.

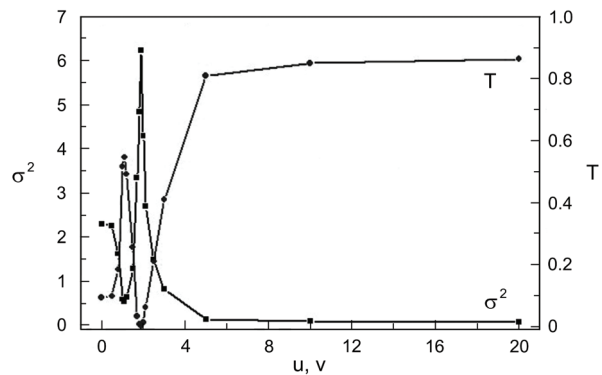


Fig. 9. Phase dispersion σ^2 and transmittance T for LC-P composite with 15 vol.% of polymer.

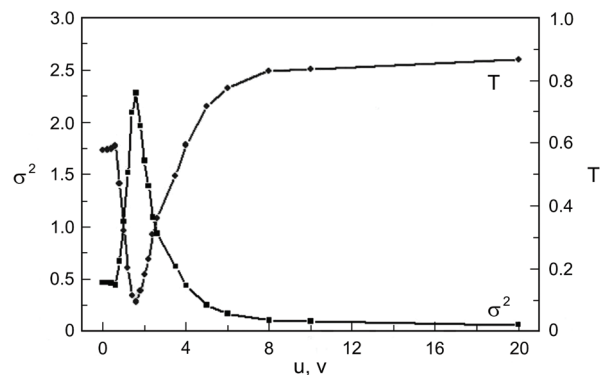


Fig. 10. Phase dispersion σ^2 and transmittance T for LC-P composite with 20 vol.% of polymer.

caused by reconstruction of polymer network while LC reorientation in the field. Such reconstruction is possible in the composites with low polymer content, when polymer network is not very strong and composite has properties of LC gel.

4. Conclusions

The methods of correlation optics are effective tools for a non-destructive study of the structure of LC–P composites. By measuring phase correlation function one can get information about the amount, size and structure of LC domains as the main scatters in these systems. The comparison with data obtained by SEM and optical microscopy confirms good reliability of the new technique. The technique can be successfully applied in the structural studies of unpowered samples as well as the samples subjected to electric field.

Acknowledgements – These studies were carried out in frame of the projects VC89 and 10-07-H of the National Academy of Sciences of Ukraine.

References

- [1] YAROSHCHUK O.V., DOLGOV L.O., KISELEV A.D., *Electro-optics and structural peculiarities of liquid crystal–nanoparticle-polymer composites*, Physical Review E **72**, 2005, p. 051715.
- [2] DOLGOV L., YAROSHCHUK O., QIU L., *SEM investigations of the polymer morphology in the liquid crystal-polymer composites with different polymer contents*, Molecular Crystals and Liquid Crystals **468**, 2007, pp. 335–344.
- [3] ANGELSKY O.V., MAKSYMYAK A.P., MAKSYMYAK P.P., HANSON S.G., *Optical correlation diagnostics of rough surfaces with large surface inhomogeneities*, Optics Express **14**(16), 2006, pp. 7299–7311.
- [4] ANGELSKY O., MAKSYMYAK P., *Optical correlation diagnostics of surface roughness in coherent-domain optical methods*, [In] *Handbook of Coherent Domain Optical Methods*, [Ed.] V. Tuchin, Chapter 2, Kluwer Academic Publishers, 2004, pp. 43–92.
- [5] RYTOV S., KRAVTSOV Yu., TATARSKY V., *Principles of Statistical Radiophysics*, Springer, Berlin, 1989.
- [6] JIN-JEI WU, CHIH-MING WANG, *Electro-optical properties of aligned polymer dispersed liquid crystal films*, Physics Letters A **232**(1–2), 1997, pp. 149–154.
- [7] BHARGAVA R., WANG S.-Q., KOENIG J.L., *FTIR imaging studies of a new two-step process to produce polymer dispersed liquid crystals*, Macromolecules **32**(8), 1999, pp. 2748–2760.
- [8] KONKOLOVICH V., PRESNYAKOV V.V., ZYRYANOV V.YA., LOIKO V.A., SHABANOV V.F., *Interference quenching of light transmitted through a monolayer film of polymer-dispersed nematic liquid crystal*, JETP Letters **71**(12), 2000, pp. 486–488.

Received January 30, 2009
in revised form March 2, 2009